

Microstructure and Mechanical Properties of Ni-Based Complex Concentrated Alloys under Radiation Environment

Qiuwei Xing^{1,*}, Xu Zhu¹, Guoju Li², Xinzhe Zhang², Xinfang Zhang¹ and Zhanxing Chen^{1,*} 

¹ School of Materials Science and Engineering, Zhengzhou University of Aeronautics, Zhengzhou 450046, China

² School of Aerospace Engineering, Zhengzhou University of Aeronautics, Zhengzhou 450046, China

* Correspondence: xqw@zua.edu.cn (Q.X.); zxchen0322@163.com (Z.C.)

Abstract: The rapid development of fusion-reactor technology calls for excellent anti-irradiation materials. Complex concentrated alloy (CCA) is a newly proposed alloy concept which is a promising candidate of nuclear fusion materials by virtue of its great phase stability under irradiation. This article summarizes anti-radiation mechanism and the microstructure evolution in HEAs. The effective factors on irradiation behavior of HEAs, including entropy, sample size and temperature, are discussed. Finally, the article introduces the potential ways to solve the economic and environmental problems which the HEAs faced for their applications in the future. In summary, the HEAs usually show better irradiation resistance than traditional alloys, such as less swelling, smaller size of defects, and more stable mechanical properties. One possible reason for the irradiation resistance of HEA is the self-healing effect induced by the high-entropy and atomic-level stress among the metal atoms. The activation of the principal element should be considered when selecting components of HEA, and the high throughput technique is a potential way to reduce the design and fabrication cost of HEAs. It is reasonable to expect that coming years will see the application of novel HEAs in fusion reactors.

Keywords: high-entropy alloy; irradiation resistance; mechanical property; fusion reactor materials



Citation: Xing, Q.; Zhu, X.; Li, G.; Zhang, X.; Zhang, X.; Chen, Z. Microstructure and Mechanical Properties of Ni-Based Complex Concentrated Alloys under Radiation Environment. *Crystals* **2022**, *12*, 1322. <https://doi.org/10.3390/cryst12091322>

Academic Editor: Shouxun Ji

Received: 18 May 2022

Accepted: 15 September 2022

Published: 19 September 2022

Publisher's Note: MDPI stays neutral with regard to jurisdictional claims in published maps and institutional affiliations.



Copyright: © 2022 by the authors. Licensee MDPI, Basel, Switzerland. This article is an open access article distributed under the terms and conditions of the Creative Commons Attribution (CC BY) license (<https://creativecommons.org/licenses/by/4.0/>).

1. Introduction

Nuclear energy is a green and sustainable power source, which can replace the fuel energy and reduce the greenhouse effect on the earth. Nowadays, about 11% of the global power supply is offered by nuclear reactors [1]. A fusion reactor is a future nuclear power source, the energy of which comes from nuclear fusion, and it may theoretically generate unlimited power with much less radiation waste. Up to now, the Tokamak is the most well-studied approach to using fusion power. Figure 1 shows a typical tokamak device, the ARIES-AT fusion power core. The high-temperature ionized plasma is magnetically confined in a toroidal magnetic field, and the first-wall materials of the device, which directly face the plasma, are irradiated by the heat high-energy neutron [2]. The development of fusion reactors puts forward higher requirements for the radiation resistance of materials because the neutron flux from high-temperature plasma is higher than from fission reactions [3].

Complex concentrated alloys (CCAs) are novel solid-solution alloys that were proposed in 2004 [4–6]. The CCAs usually consist of four or more principal elements, and the content of each component is more than 5% [7–9]. The simple solid solution phases of CCAs are stabilized by the high configurational entropy among the principal elements. By virtue of special phase structure and cocktail effect of multiple principal elements, the CCAs are reported to show outstanding properties such as abnormal mechanical properties, excellent thermal stability, good corrosion resistance and high wear resistance [10–14]. Recently, the irradiation resistance of CCAs attracts extension interest in the materials community due to their good swelling tolerance and stable mechanical properties under irradiation.

One possible reason for the excellent irradiation resistance of CCA is the self-healing effect induced by atomic-level stress among metal atoms.

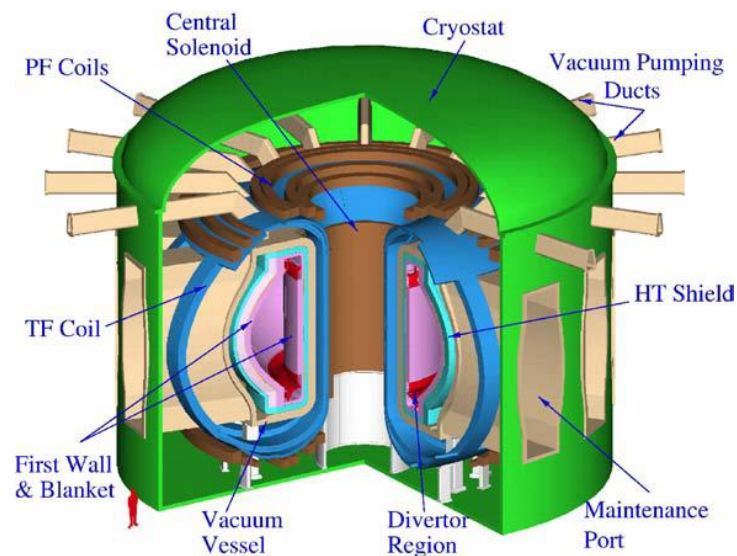


Figure 1. The ARIES-AT fusion power core, reprinted with permission from Ref. [15]. The materials of first wall suffer strong neutron flux.

This article reviews the recent progress of irradiation-resistant CCAs and introduces the irradiation behaviors of CCAs, including the evolution of their microstructures and mechanical properties under different irradiation conditions, and summarizes their anti-irradiation mechanism under different conditions.

2. The Microstructure Evolution of CCA under Irradiation

The recombination of radiation-induced vacancies and interstitials is the key point to good irradiation tolerance [16]. This section briefly introduces the anti-radiation mechanism in CCAs and reviews their microstructure evolution under irradiation.

2.1. The Anti-Radiation Mechanism in CCA

Early in 2013, the high electron-irradiation damage tolerance was observed in near equal atomic Zr-Hf-Nb alloys [17]. Egami et al. [18] explained the anti-radiation mechanism of Zr-Hf-Nb by calculating their atomic-level stress using the density functional theory (DFT), and predicted the high irradiation resistance of CCA. The atomic-level pressure of CCAs derives from the intrinsic atomic size differences and the electronegativity [19], and it can be defined as:

$$p_i = \frac{1}{3} (\sigma_i^{xx} + \sigma_i^{yy} + \sigma_i^{zz}), \quad (1)$$

$$\sigma_i^{\alpha\beta} = \frac{1}{V_i} \sum_j f_{ij}^{\alpha} r_{ij}^{\beta}, \quad (2)$$

where $\sigma_i^{\alpha\beta}$ is atomic-level stress tensor of the i th atom, α and β are Cartesian coordinates, V_i is the atomic volume of the i th atom, and f_{ij}^{α} and r_{ij}^{β} are the two-body force and the distance between the atoms i and j . Egami et al. [18] speculate that CCAs with the atomic-level volume strain close to 0.1 are self-healing and highly irradiation resistant. Tong et al. [20] revealed the local lattice distortion can be relaxed by lattice expansion in FeCoNiCr and FeCoNiCrMn under low dose irradiation.

2.2. The Defect of CCA under Radiation

The lattice atom leaves the initial position after being bombarded by high-energy particles when alloys are subjected to irradiation, and results in the generation of a Frenkel pair.

The accumulation and translocation of Frenkel pairs lead to the formation of complex defect structures, such as point defect and line defect stacking defect tetrahedrons, dislocation loops, precipitations, voids and He bubbles [21]. The defect growing in CCA is restrained due to the self-healing effect, resulting in better irradiation resistance of CCA than conventional alloys. Figure 2 displays the dislocation loops distribution in nickel-based CCAs after irradiation. The alloys show denser and smaller dislocation loops with the increasing mixing entropy. The single phase $\text{Al}_{0.1}\text{CoCrFeNi}$ exhibits great structure stability against precipitate at ~ 43 dpa 3 MeV Au ion irradiation [22]. The stable stacking fault tetrahedron forms in FeCrCoNi CCA under the high dose 1.5 MeV Ni ion irradiation [23]. Compared with 304 SS and pure nickel, the CrMnFeCoNi CCA exhibits smallest helium bubble size and densest stacking fault tetrahedron [24]. The vacancy formation is also difficult in CCA. Xu et al. [25] studied the formation of vacancy clusters in CoCrFeMnNi CCA using first principle calculation and experiment, and found it is difficult to form tri-vacancy clusters, which is the reason for the good irradiation resistance of CCA.

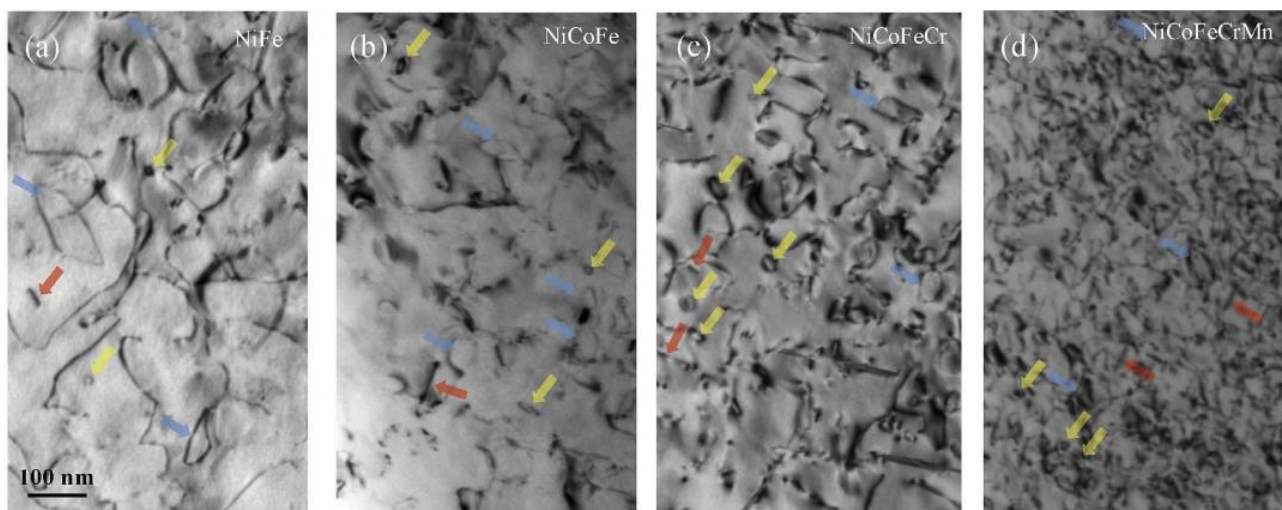


Figure 2. The dislocation loops evolution with the compositional complexity of composition in Ni-based CCAs, reprinted with permission from Ref. [26].

3. Mechanical Properties of CCA under Irradiation

The materials with irradiation defects, such as helium bubbles, irradiation hardening and embrittlement, lead to the deterioration of mechanical properties such as strength and toughness of materials and even failure, which seriously affects the safety of fusion reactors. The nanostructures, such as precipitation and matrix damage induced by radiation, hinder the dislocation slip and increase plastic deformation stress in CCA. As the result, the alloys often show hardening and embrittlement after being irradiated. Figure 3 shows the temperature dependence of mechanical properties of Ni-based CCAs. The yield and ultimate strengths of NiCoCr, NiCoCrMn and FeNiCoCr have stronger temperature dependence than NiCo and Ni, and the nature of the constituent elements can also affect the mechanical properties of CCAs [27].

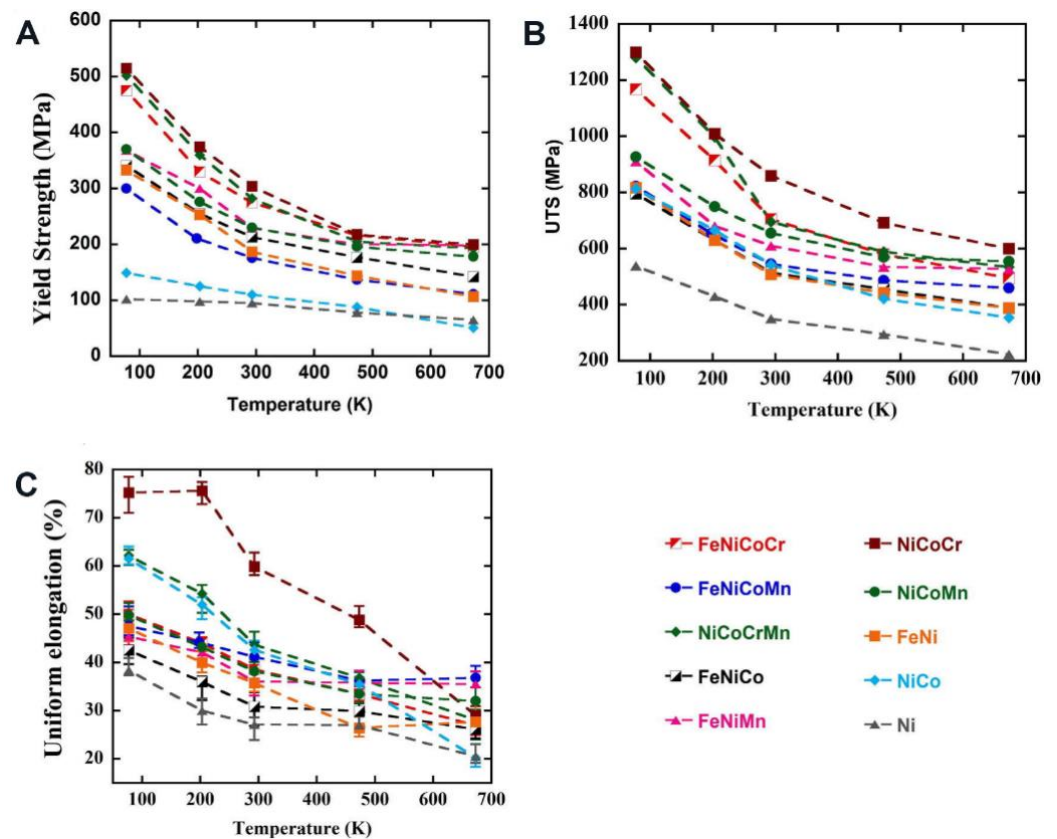


Figure 3. Temperature dependence of (A) yield stress, (B) ultimate tensile stress and (C) uniform elongation to fracture for equal atomic alloys and Ni, reprinted with permission from Ref. [27].

The hardening is a common phenomenon in CCAs after irradiated, the reason of which can be attributed to the irradiation-induced lattice damage and the defect formation. For example, the hardness of CrMnFeCoNi is measured higher after irradiation at room temperature [24]. The CoCrFeCuNi CCA exhibits notable hardening when irradiated with a 100 keV He⁺ ion beam, due to the dislocation-dominated hardening effect [28]. However, the hardness of some CCAs have no big change after being irradiated. The Ti₂ZrHfV_{0.5}Mo_{0.2} CCA designed by Lu et al. [29] shows almost no hardening after helium ion irradiation.

Chen et al. [30] studied the helium bubble formation in CCA, which is the reason for the helium embrittlement of nuclear structural materials. They found the helium bubble size in FeCoNiCr CCA is smaller than in pure nickel and steel. However, the hardness of V_{2.5}Cr_{1.2}WmoCo_{0.04} CCA decreases when irradiated at low temperature [31]. Jawaharram et al. [32] measured irradiation-induced creep during 2.6 MeV Ag ion irradiation. The irradiation induced creep enters the sink-limited regime at about 100 °C when the grain size is smaller than 80 nm, and the creep compliance scales inversely with grain size.

4. Effective Factors on Irradiation Resistance of CCA

The irradiation CCAs need to present different shapes and compositions to suit the complex serving environment in fusion reactors and their irradiation performance can be affected by different conditions. This section discusses three attractive factors which are effective on irradiation resistance of CCA, including alloying, irradiation of CCA films and high-temperature irradiation on CCAs.

4.1. Effect of Alloying

The contribution of entropy to irradiation properties is an interest in CCAs research because high mixing entropy is a common characteristic of CCAs. The mixing entropy of CCAs can be defined as [33]:

$$\Delta S_{mix} = -R \sum_{i=1}^n (c_i \ln c_i), \quad (3)$$

where the c_i is mole percent of i th component in the alloy system, and R is the gas constant, and n is the component number. According to Equation (3), it is easy to know that the increase of component number can magnify the mixing entropy in CCAs. Therefore, the entropy effect of multi-component alloy is notably higher than pure metals. In this way, Chen et al. [34] compared He-bubble-formation resistance of FeCoNiCr alloy with pure nickel. The CCA shows lower He bubble volume fraction than the nickel. Li et al. [35] simulated the response of CoNiCrFeMn to nickel-atom bombardment via the molecular dynamics method. The CCA has less dispersed point defect and can tolerate more bombardment than pure nickel. These results prove the CCAs are more stable than pure nickel under irradiation, and further research revealed the irradiation behaviour evolution of CCAs with the increased component number.

Lu et al. [26] irradiated a series of single-phase Ni-based CCAs, including NiFe, NiCoFe, NiCoFeCr and NiCoFeCrMn, with 3 MeV Ni²⁺ ions, and observed a higher fraction of faulted loops in the alloys with more components, indicating the increasing compositional complexity extends the incubation period and delay loop growth. Jin et al. [36] studied the swelling of pure nickel and six Ni-based CCAs, and found the swelling of nickel-contained alloy greatly depends on the compositional complexity of the alloys (Figure 4a). However, the hardness has no-liner relationship with configuration entropy. The NiCo binary alloy show about two times higher hardness than others (Figure 4b). Zhang et al. [37] studied the effects of dose and temperature on void swelling in NiCoFeCr CCAs, they found defect diffusion and radiation-induced segregation are affected by chemical complexity. The Ab-initio MD simulations of interstitial atoms diffusion in Ni-based CCAs indicated the diffusion occurs through preferential elements in CCAs, which have influence on the phase stabilities under radiation [38].

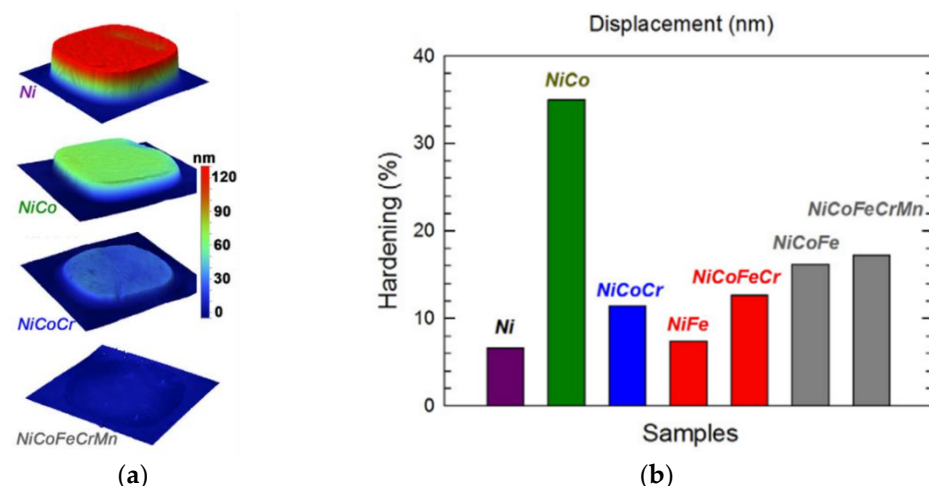


Figure 4. The swelling and hardening of the nickel-contained equal atomic alloys (a) the swelling (b) the hardening, Reprinted/adapted with permission from Ref. [36].

Besides the high-entropy effect caused by the component group, the addition of single element also has influence on irradiation behavior, which commonly comes with the transformation of microstructure. For example, the phase structure of Al_xCoCrFeNi CCA can transform from fcc structure to bcc structure with the increasing content of Al [39], so the irradiation behavior of Al_xCoCrFeNi greatly depends on the atomic percent of aluminum.

The single fcc phase $\text{Al}_{0.1}\text{CoCrFeNi}$ CCA shows great phase stability against ~ 43 dpa 3 eV Au ion irradiation, whereas multiple phase CCA exhibits significant precipitation under identical condition [22]. Furthermore, the defect clusters in disordered bcc and fcc phases are found to be smaller than the ordered B2 phase under irradiation according to the comparison between $\text{Al}_{0.75}\text{CoCrFeNi}$ and $\text{Al}_{1.5}\text{CoCrFeNi}$ [40].

4.2. Effect of Sample Size

The CCAs can be divided into bulk CCAs, CCA films, CCA wires and CCA powders according to the dimension of their shapes [41]. The small size CCA may form nanocrystalline or amorphous phases due to the increased cooling rate during fabrication, so the low dimensional CCAs show different properties with bulk CCAs. Recently, the irradiation resistance of CCA films draws research interests due to their fine microstructures. For example, the swelling resistance of $\text{Al}_{1.5}\text{CoCrFeNi}$ CCA film [42] is better than bulk CCA materials, because the effect of ultra-fine nano-crystalline reduces the He cluster. Zhang et al. [43] compared the thermal-induced and irradiation-induced grain growth in nanocrystalline NiFeCoCrCu CCA films, and the fcc phase of CCA film is stable when grain grows under the irradiation. Zhang et al. [44] investigated the interface stabilities and mechanical properties of AlCrMoNbZr/(AlCrMoNbZr)N multilayer CCA coating under helium ion irradiations. The multilayer CCA coatings show sharp interfaces between different layers and form no helium bubbles after being irradiated. The crystallization occurs in amorphous AlCrFeMoTi CCA coating after irradiated by 6 MeV Au ion beam at high dose. The hardness of AlCrFeMoTi CCA coating increases obviously with the increasing irradiation dose [45].

4.3. Effect of Temperature

The CCAs are reported to have fascinating properties at elevated temperatures, such as excellent thermal stability, high yield strength and softening resistance, high wear resistance, etc. The structural stability of CCAs at high temperatures derives from the low Gibbs energy reduced by mixing entropy. The mixing Gibbs free energy of CCA can be expressed as [46]:

$$\Delta G_{mix} = \Delta H_{mix} - T\Delta S_{mix}, \quad (4)$$

here ΔH_{mix} is the mixing enthalpy, ΔS_{mix} is the mixing entropy, and T is the absolute temperature. According to Equation 4, the increasing temperature can magnify the effect of entropy and reduce the Gibbs free energy of system, stabilizing solid solution in CCAs.

Yang et al. [47] compared He-ion irradiation resistance of CCA CrMnFeCoNi with pure nickel and 304 SS at 450 °C, found the CCA has the best He-ion irradiation resistance, due to the low He atom and point defect mobility. Yang et al. [48,49] studied the irradiation response of $\text{Al}_{0.1}\text{CoCrFeNi}$ and $\text{Al}_{0.3}\text{CoCrFeNi}$ under 3 MeV Au ion irradiation at elevated temperatures. The CCAs show no obvious phase transformation under high-temperature ion irradiation, and the defect size increases when defect density decreases with the increasing temperature in $\text{Al}_{0.1}\text{CoCrFeNi}$ (Figure 5). The dislocation loops of $\text{Al}_{0.3}\text{CoCrFeNi}$ under irradiation transforms from predominantly faulted $1/3\{1\ 1\ 1\}$ dislocation loops to a mixture of faulted $1/3\{1\ 1\ 1\}$ dislocation loops and perfect loops when the temperature increase to 500 °C. Chen et al. [50] compared $\text{Al}_{0.3}\text{CoCrFeNi}$ and CoCrFeMnNi with 316H SS at 300 °C with 1 MeV krypton ions to 1 dpa, and found the irradiation behaviors of CCAs are similar to SS. The hardness of CrMnFeCoNi CCA is enhanced under helium ion irradiation at 450 °C due to the increasing helium bubble size inside alloy [24]. Liu et al. [51] studied the He-induced cavities evolution of nickel-contained equal atomic alloys at 673, 773, 873 and 973 K, and found the increased component number can suppress the growth of He cavities at 673 K.

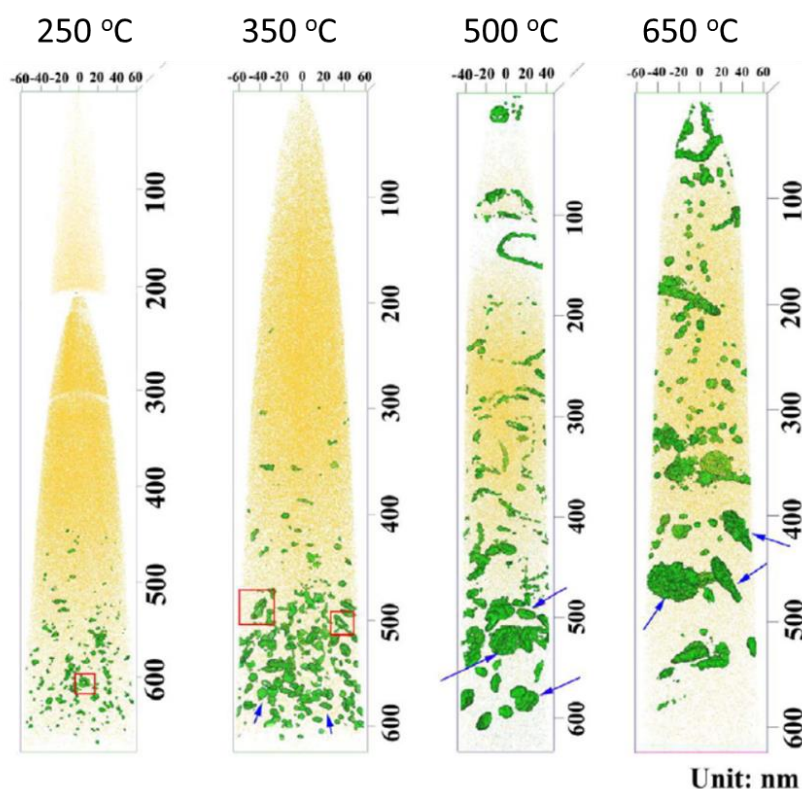


Figure 5. The dislocation loops in $\text{Al}_{0.1}\text{CoCrFeNi}$ CCA when irradiated under 3 MeV Au ion beam at 250, 350, 500 and 650 °C is characterized by atom probe tomography (APT). The size and density of dislocation loops grows with the irradiation temperature, reprinted with permission from Ref. [49].

5. Future Trend

Although the researches on the irradiation of CCA have achieved a series of inspiring results, most of the CCA can rarely serve as nuclear materials. Now the application of CCAs on the fusion reactor mainly faced two big problems: low economic efficiency and high radio activation.

5.1. Low Activation

The metal atoms are bombarded by the neutrons and generate the radio-active isotopes inevitably when the alloys serve as fusion reactor materials. The long half-life period of radioactive isotopes will increase the difficulties and cost to deal with these materials after their service. Because the spent fuels of fusion reaction are negligible, the radiation waste of fusion reactor mainly comes from the induced-radioactive materials. The low-activation alloys, which mainly consist of short or medium lived metals, can reduce radiation pollution and are more unfriendly to the environment. Therefore, the constituent elements of ideal CCA should not only have a small atomic radius difference to form a solid solution matrix, but also have low induced radioactivity. However, many CCAs contain undesirable high-activation metals, such as cobalt, which can produce ^{60}Co via neutron-induced transmutation [52]. The low-activation metals are preferred to be selected as principal elements of CCAs when designed as fusion reactor materials. For instance, the low activation CCA of TiVZrTa and TiVCrTa show comparable mechanical properties and increased irradiation resistance when compared with TiVNbTa [53]. After removing the high-activation element cobalt in Cantor alloy, the medium entropy alloy FeCrNiMn shows similar mechanical strength and phase stability to Fe-Cr-Ni, and its tensile mechanical performance is comparable to SS at 60 °C up to 0.1 and 1 dpa neutron irradiation [54]. Zhang et al. [55] designed low-activation $\text{VCrFeTa}_x\text{W}_x$ ($x = 0.1, 0.2, 0.3, 0.4, \text{ and } 1$) CCA, and $\text{VcrFeTa}_{0.1}\text{W}_{0.1}$ and $\text{VcrFeTa}_{0.2}\text{W}_{0.2}$ present excellent heat-softening resistance from 600 to 800 °C. The reduced-activity CCA of HfTaTiVZr shows stable microstructure with

high hardness [56], the radiation-induced hardening of which is lower than SS under the same irradiation conditions due to the self-healing effect of CCAs [57].

5.2. Low Cost

The CCAs are promising irradiation-resistant materials, whereas their applications are limited by economic efficiency. The cost of CCAs mainly comes from raw materials and the processing of the preparation.

Firstly, the minor additions of rare metals are common in traditional alloys and have acceptable influence on the alloy price because the contents of these high-cost elements are small. The material costs of alloys are considerable when rare metal plays a role as a principal component. Although a great number of CCAs are designed to achieve as high mixing entropy as possible, recent research shows that the properties of CCAs have a non-linear relationship with the mixing entropy [47]. The development of non-equal atomic CCAs partly solves this problem. For example, the high entropy steels (HESs) contain more iron than normal high-entropy alloys, and the $\text{Fe}_{50}\text{Mn}_{30}\text{Co}_{10}\text{Cr}_{10}$ HESs overcome the trade-off between strength and ductility due to the transformation-induced plasticity (TRIP) [58]. The increased content of cheap elements, such as iron, greatly reduced the total cost of raw materials of CCAs.

The second cost comes from the development and preparation of novel CCAs, especially when searching the best combination of the principal elements. The high-throughput technology, which is widely applied to the fabrication of materials, is a potential way to reduce processing cost of CCAs. For example, Li et al. prepared Al-Zn-Li-Mg-Cu light-weight entropic alloy [59] and $\text{Al}_x\text{CoCrFeNi}$ ($x = 0, 0.3, 0.5, 0.75$ and 1) CCAs [60] with gradient grain size using super-gravity method. The co-sputtering technique can be applied to phase screening of (CrFeV)-(TaW) low-activation CCA films [61] (Figure 6). Parkin et al. [62] investigated the phase composition of for two potential radiation damage tolerant CCA systems via high-throughput technique. They built the compositional library via co-sputtering method, mapped the phase composition on the co-sputtered films, and found the composition with a single-phase structure successfully.

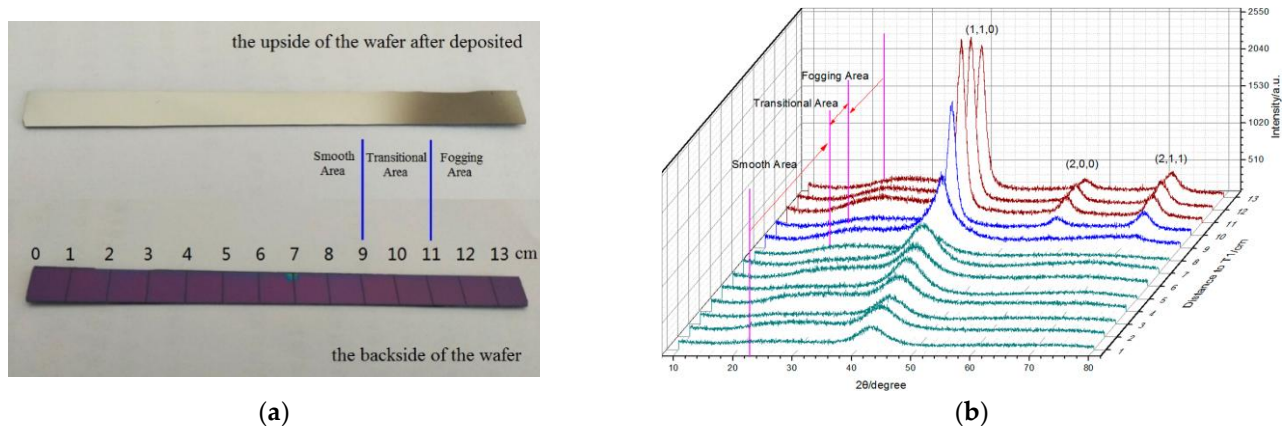


Figure 6. Microstructure evolution of CCAs fabricated by high-throughput technique: (a) The gradient (CrFeV)-(TaW) low-activation film after co-sputtering; (b) The phase evolution of (CrFeV)-(TaW) low-activation CCA films prepared by co-sputtering, reprinted with permission from Ref. [61].

6. Summaries

The CCAs have broad application prospects with the growing nuclear industry and can fulfill the future requirement of anti-irradiation materials. In this paper, the microstructure and mechanical property evolution of CCAs under irradiation are reviewed, and three factors that are effective on irradiation behavior of CCAs, including entropy, size effect and temperature, are discussed. In summary, the four core effects play different roles in irradiation behavior of CCAs: the high-entropy effect, or so-called compositional complexity, can

greatly reduce the swelling of CCAs; the element addition can bring about adjustments of irradiation resistance of CCA due to the cocktail effect; the sluggish diffusion stabilizes the microstructure of CCAs under irradiation; the lattice distortion increases the atomic level stress, result in the self-healing effect in CCAs. The new generation of CCAs will be more environment-friendly and cost-effective and they are promising for the application in fusion reactor materials in the future.

Author Contributions: Writing—original draft preparation, Q.X.; writing—review and editing, Q.X., Z.C., G.L., X.Z. (Xinzhe Zhang), X.Z. (Xinfang Zhang) and X.Z. (Xu Zhu); funding acquisition, Z.C. All authors have read and agreed to the published version of the manuscript.

Funding: This work was supported by the National Natural Science Foundation of China (No. 52001283), Key Technologies Research and Development Program of Henan Province of China (No. 212102210109, 212102210447, 222102230041).

Informed Consent Statement: Not applicable.

Data Availability Statement: Not applicable.

Acknowledgments: This work was supported by the National Natural Science Foundation of China (No.52001283), Key Technologies Research and Development Program of Henan Province of China (No. 212102210109, 212102210447, 222102230041).

Conflicts of Interest: The authors declare no conflict of interest.

References

1. Busby, J.T. *Overview of Structural Materials in Water-Cooled Fission Reactors*; Elsevier Inc.: Amsterdam, The Netherlands, 2019; ISBN 9780123970466.
2. Zinkle, S.J.; Snead, L.L. Designing Radiation Resistance in Materials for Fusion Energy. *Annu. Rev. Mater. Res.* **2014**, *44*, 241–267. [[CrossRef](#)]
3. Zinkle, S.J.; Busby, J.T. Structural materials for fission & fusion energy. *Mater. Today* **2009**, *12*, 12–19.
4. Ranganathan, S. Alloyed pleasures: Multimetallurgical cocktails. *Curr. Sci.* **2003**, *85*, 1404–1406.
5. Yeh, J.W.; Chen, S.K.; Lin, S.J.; Gan, J.Y.; Chin, T.S.; Shun, T.T.; Tsau, C.H.; Chang, S.Y. Nanostructured high-entropy alloys with multiple principal elements: Novel alloy design concepts and outcomes. *Adv. Eng. Mater.* **2004**, *6*, 299–303+274. [[CrossRef](#)]
6. Cantor, B.; Chang, I.T.H.; Knight, P.; Vincent, A.J.B. Microstructural development in equiatomic multicomponent alloys. *Mater. Sci. Eng. A* **2004**, *375–377*, 213–218. [[CrossRef](#)]
7. Yeh, J.W. Alloy design strategies and future trends in high-entropy alloys. *JOM* **2013**, *65*, 1759–1771. [[CrossRef](#)]
8. Yeh, J.W. Physical Metallurgy of High-Entropy Alloys. *JOM* **2015**, *67*, 2254–2261. [[CrossRef](#)]
9. Yeh, J.W.; Chen, Y.L.; Lin, S.J.; Chen, S.K. High-entropy alloys—A new era of exploitation. *Mater. Sci. Forum* **2007**, *560*, 1–9. [[CrossRef](#)]
10. Xu, D.; Wang, M.; Li, T.; Wei, X.; Lu, Y. A critical review of the mechanical properties of CoCrNi-based medium-entropy alloys. *Microstructures* **2022**, *2*, 2022001. [[CrossRef](#)]
11. Zhang, W.; Liaw, P.K.; Zhang, Y. Science and technology in high-entropy alloys. *Sci. China Mater.* **2018**, *61*, 2–22. [[CrossRef](#)]
12. Ye, Y.F.; Wang, Q.; Lu, J.; Liu, C.T.; Yang, Y. High-entropy alloy: Challenges and prospects. *Mater. Today* **2016**, *19*, 349–362. [[CrossRef](#)]
13. Gludovatz, B.; Hohenwarter, A.; Catoor, D.; Chang, E.H.; George, E.P.; Ritchie, R.O. A fracture-resistant high-entropy alloy for cryogenic applications. *Science* **2014**, *345*, 1153–1158. [[CrossRef](#)] [[PubMed](#)]
14. Zhang, Y.; Zuo, T.T.; Tang, Z.; Gao, M.C.; Dahmen, K.A.; Liaw, P.K.; Lu, Z.P. Microstructures and properties of high-entropy alloys. *Prog. Mater. Sci.* **2014**, *61*, 1–93. [[CrossRef](#)]
15. Najmabadi, F.; Abdou, A.; Bromberg, L.; Brown, T.; Chan, V.C.; Chu, M.C.; Dahlgren, F.; El-Guebaly, L.; Heitzenroeder, P.; Henderson, D.; et al. The ARIES-AT advanced tokamak, Advanced technology fusion power plant. *Fusion Eng. Des.* **2006**, *80*, 3–23. [[CrossRef](#)]
16. Beyerlein, I.J.; Caro, A.; Demkowicz, M.J.; Mara, N.A.; Misra, A.; Uberuaga, B.P. Radiation damage tolerant nanomaterials. *Mater. Today* **2013**, *16*, 443–449. [[CrossRef](#)]
17. Nagase, T.; Anada, S.; Rack, P.D.; Noh, J.H.; Yasuda, H.; Mori, H.; Egami, T. MeV electron-irradiation-induced structural change in the bcc phase of Zr-Hf-Nb alloy with an approximately equiatomic ratio. *Intermetallics* **2013**, *38*, 70–79. [[CrossRef](#)]
18. Egami, T.; Guo, W.; Rack, P.D.; Nagase, T. Irradiation Resistance of Multicomponent Alloys. *Metall. Mater. Trans. A* **2014**, *45*, 180–183. [[CrossRef](#)]
19. Egami, T.; Ojha, M.; Khorgolkhuu, O.; Nicholson, D.M.; Stocks, G.M. Local Electronic Effects and Irradiation Resistance in High-Entropy Alloys. *JOM* **2015**, *67*, 2345–2349. [[CrossRef](#)]

20. Tong, Y.; Velisa, G.; Zhao, S.; Guo, W.; Yang, T.; Jin, K.; Lu, C.; Bei, H.; Ko, J.Y.P.; Pagan, D.C.; et al. Evolution of local lattice distortion under irradiation in medium- and high-entropy alloys. *Materialia* **2018**, *2*, 73–81. [[CrossRef](#)]
21. Zhang, X.; Hattar, K.; Chen, Y.; Shao, L.; Li, J.; Sun, C.; Yu, K.; Li, N.; Taheri, M.L.; Wang, H.; et al. Radiation damage in nanostructured materials. *Prog. Mater. Sci.* **2018**, *96*, 217–321. [[CrossRef](#)]
22. Yang, T.; Xia, S.; Liu, S.; Wang, C.; Liu, S.; Fang, Y.; Zhang, Y.; Xue, J.; Yan, S.; Wang, Y. Precipitation behavior of Al_xCoCrFeNi high entropy alloys under ion irradiation. *Sci. Rep.* **2016**, *6*, 32146. [[CrossRef](#)] [[PubMed](#)]
23. Abhaya, S.; Rajaraman, R.; Kalavathi, S.; David, C.; Panigrahi, B.K.; Amarendra, G. Effect of dose and post irradiation annealing in Ni implanted high entropy alloy FeCrCoNi using slow positron beam. *J. Alloys Compd.* **2016**, *669*, 117–122. [[CrossRef](#)]
24. Yang, L.; Ge, H.; Zhang, J.; Xiong, T.; Jin, Q.; Zhou, Y.; Shao, X.; Zhang, B.; Zhu, Z.; Zheng, S.; et al. High He-ion irradiation resistance of CrMnFeCoNi high-entropy alloy revealed by comparison study with Ni and 304SS. *J. Mater. Sci. Technol.* **2019**, *35*, 300–305. [[CrossRef](#)]
25. Xu, Q.; Guan, H.Q.; Zhong, Z.H.; Huang, S.S.; Zhao, J.J. Irradiation resistance mechanism of the CoCrFeMnNi equiatomic high-entropy alloy. *Sci. Rep.* **2021**, *11*, 608. [[CrossRef](#)]
26. Lu, C.; Yang, T.; Jin, K.; Gao, N.; Xiu, P.; Zhang, Y.; Gao, F.; Bei, H.; Weber, W.J.; Sun, K.; et al. Radiation-induced segregation on defect clusters in single-phase concentrated solid-solution alloys. *Acta Mater.* **2017**, *127*, 98–107. [[CrossRef](#)]
27. Wu, Z.; Bei, H.; Pharr, G.M.; George, E.P. Temperature dependence of the mechanical properties of equiatomic solid solution alloys with face-centered cubic crystal structures. *Acta Mater.* **2014**, *81*, 428–441. [[CrossRef](#)]
28. Wang, Y.; Zhang, K.; Feng, Y.; Li, Y.; Tang, W.; Wei, B. Evaluation of radiation response in CoCrFeCuNi high-entropy alloys. *Entropy* **2018**, *20*, 835. [[CrossRef](#)]
29. Lu, Y.; Huang, H.; Gao, X.; Ren, C.; Gao, J.; Zhang, H.; Zheng, S.; Jin, Q.; Zhao, Y.; Lu, C.; et al. A promising new class of irradiation tolerant materials: Ti₂ZrHfV_{0.5}Mo_{0.2} high-entropy alloy. *J. Mater. Sci. Technol.* **2019**, *35*, 369–373. [[CrossRef](#)]
30. Chen, D.; Tong, Y.; Li, H.; Wang, J.; Zhao, Y.L.; Hu, A.; Kai, J.J. Helium accumulation and bubble formation in FeCoNiCr alloy under high fluence He⁺ implantation. *J. Nucl. Mater.* **2018**, *501*, 208–216. [[CrossRef](#)]
31. Patel, D.; Richardson, M.D.; Jim, B.; Akhmaliev, S.; Goodall, R.; Gandy, A.S. Radiation damage tolerance of a novel metastable refractory high entropy alloy V_{2.5}Cr_{1.2}WMoCo_{0.04}. *J. Nucl. Mater.* **2020**, *531*, 152005. [[CrossRef](#)]
32. Jawaharram, G.S.; Barr, C.M.; Monterrosa, A.M.; Hattar, K.; Averbach, R.S.; Dillon, S.J. Irradiation induced creep in nanocrystalline high entropy alloys. *Acta Mater.* **2020**, *182*, 68–76. [[CrossRef](#)]
33. Yang, X.; Zhang, Y. Prediction of high-entropy stabilized solid-solution in multi-component alloys. *Mater. Chem. Phys.* **2012**, *132*, 233–238. [[CrossRef](#)]
34. Chen, D.; Zhao, S.; Sun, J.; Tai, P.; Sheng, Y.; Zhao, Y.; Yeli, G.; Lin, W.; Liu, S.; Kai, W.; et al. Diffusion controlled helium bubble formation resistance of FeCoNiCr high-entropy alloy in the half-melting temperature regime. *J. Nucl. Mater.* **2019**, *526*, 151747. [[CrossRef](#)]
35. Li, Y.; Li, R.; Peng, Q. Enhanced surface bombardment resistance of the CoNiCrFeMn high entropy alloy under extreme irradiation flux. *Nanotechnology* **2020**, *31*, 025703. [[CrossRef](#)]
36. Jin, K.; Lu, C.; Wang, L.M.; Qu, J.; Weber, W.J.; Zhang, Y.; Bei, H. Effects of compositional complexity on the ion-irradiation induced swelling and hardening in Ni-containing equiatomic alloys. *Scr. Mater.* **2016**, *119*, 65–70. [[CrossRef](#)]
37. Fan, Z.; Yang, T.N.; Kombariah, B.; Wang, X.; Edmondson, P.D.; Osetsky, Y.N.; Jin, K.; Lu, C.; Bei, H.; Wang, L.; et al. From suppressed void growth to significant void swelling in NiCoFeCr complex concentrated solid-solution alloy. *Materialia* **2020**, *9*, 100603. [[CrossRef](#)]
38. Zhao, S.; Osetsky, Y.; Zhang, Y. Preferential diffusion in concentrated solid solution alloys: NiFe, NiCo and NiCoCr. *Acta Mater.* **2017**, *128*, 391–399. [[CrossRef](#)]
39. Wang, W.-R.; Wang, W.-L.; Wang, S.-C.; Tsai, Y.-C.; Lai, C.-H.; Yeh, J.-W. Effects of Al addition on the microstructure and mechanical property of Al_xCoCrFeNi high-entropy alloys. *Intermetallics* **2012**, *26*, 44–51. [[CrossRef](#)]
40. Xia, S.; Gao, M.C.; Yang, T.; Liaw, P.K.; Zhang, Y. Phase stability and microstructures of high entropy alloys ion irradiated to high doses. *J. Nucl. Mater.* **2016**, *480*, 100–108. [[CrossRef](#)]
41. Zhang, Y.; Xing, Q. High Entropy Alloys: Manufacturing Routes. In *Encyclopedia of Materials: Metals and Alloys*; Elsevier: Amsterdam, The Netherlands, 2022; pp. 327–338.
42. Pu, G.; Lin, L.; Ang, R.; Zhang, K.; Liu, B.; Liu, B.; Peng, T.; Liu, S.; Li, Q. Outstanding radiation tolerance and mechanical behavior in ultra-fine nanocrystalline Al_{1.5}CoCrFeNi high entropy alloy films under He ion irradiation. *Appl. Surf. Sci.* **2020**, *516*, 146129. [[CrossRef](#)]
43. Zhang, Y.; Tunes, M.A.; Crespillo, M.L.; Zhang, F.; Boldman, W.L.; Rack, P.D.; Jiang, L.; Xu, C.; Greaves, G.; Donnelly, S.E.; et al. Thermal stability and irradiation response of nanocrystalline CoCrCuFeNi high-entropy alloy. *Nanotechnology* **2019**, *30*, 294004. [[CrossRef](#)]
44. Zhang, W.; Wang, M.; Wang, L.; Liu, C.H.; Chang, H.; Yang, J.J.; Liao, J.L.; Yang, Y.Y.; Liu, N. Interface stability, mechanical and corrosion properties of AlCrMoNbZr/(AlCrMoNbZr)N high-entropy alloy multilayer coatings under helium ion irradiation. *Appl. Surf. Sci.* **2019**, *485*, 108–118. [[CrossRef](#)]
45. Yang, J.; Shi, K.; Chen, Q.; Zhang, W.; Zhu, C.; Ning, Z.; Liao, J.; Yang, Y.; Liu, N.; Yang, J. Effect of Au-ion irradiation on the surface morphology, microstructure and mechanical properties of amorphous AlCrFeMoTi HEA coating. *Surf. Coatings Technol.* **2021**, *418*, 127252. [[CrossRef](#)]

46. Zhang, Y.; Zhou, Y.J.; Lin, J.P.; Chen, G.L.; Liaw, P.K. Solid-solution phase formation rules for multi-component alloys. *Adv. Eng. Mater.* **2008**, *10*, 534–538. [[CrossRef](#)]
47. Xia, S.; Lousada, C.M.; Mao, H.; Maier, A.C.; Korzhavyi, P.A.; Sandström, R.; Wang, Y.; Zhang, Y. Nonlinear oxidation behavior in pure Ni and Ni-containing entropic alloys. *Front. Mater.* **2018**, *5*, 53. [[CrossRef](#)]
48. Yang, T.; Guo, W.; Poplawsky, J.D.; Li, D.; Wang, L.; Li, Y.; Hu, W.; Crespillo, M.L.; Yan, Z.; Zhang, Y.; et al. Structural damage and phase stability of Al_{0.3}CoCrFeNi high entropy alloy under high temperature ion irradiation. *Acta Mater.* **2020**, *188*, 1–15. [[CrossRef](#)]
49. Yang, T.; Xia, S.; Guo, W.; Hu, R.; Poplawsky, J.D.; Sha, G.; Fang, Y.; Yan, Z.; Wang, C.; Li, C.; et al. Effects of temperature on the irradiation responses of Al_{0.1}CoCrFeNi high entropy alloy. *Scr. Mater.* **2018**, *144*, 31–35. [[CrossRef](#)]
50. Chen, W.Y.; Liu, X.; Chen, Y.; Yeh, J.W.; Tseng, K.K.; Natesan, K. Irradiation effects in high entropy alloys and 316H stainless steel at 300 °C. *J. Nucl. Mater.* **2018**, *510*, 421–430. [[CrossRef](#)]
51. Liu, S.; Lin, W.; Chen, D.; Han, B.; Zhao, S.; He, F.; Niu, H.; Kai, J. Effects of temperature on helium cavity evolution in single-phase concentrated solid-solution alloys. *J. Nucl. Mater.* **2021**, *557*, 153261. [[CrossRef](#)]
52. Zinkle, S.J. *Advanced Irradiation-Resistant Materials for Generation IV Nuclear Reactors*; Elsevier Ltd.: Amsterdam, The Netherlands, 2017; ISBN 9780081009123.
53. Kareer, A.; Waite, J.C.; Li, B.; Couet, A.; Armstrong, D.E.J.; Wilkinson, A.J. Short communication: ‘Low activation, refractory, high entropy alloys for nuclear applications’. *J. Nucl. Mater.* **2019**, *526*, 151744. [[CrossRef](#)]
54. Li, C.; Hu, X.; Yang, T.; Kumar, N.K.; Wirth, B.D.; Zinkle, S.J. Neutron irradiation response of a Co-free high entropy alloy. *J. Nucl. Mater.* **2019**, *527*, 151838. [[CrossRef](#)]
55. Zhang, W.; Liaw, P.K.; Zhang, Y. A novel low-activation VCrFeTaxWx (x = 0.1, 0.2, 0.3, 0.4, and 1) high-entropy alloys with excellent heat-softening resistance. *Entropy* **2018**, *20*, 951. [[CrossRef](#)] [[PubMed](#)]
56. Ayyagari, A.; Salloom, R.; Muskeri, S.; Mukherjee, S. Low activation high entropy alloys for next generation nuclear applications. *Materialia* **2018**, *4*, 99–103. [[CrossRef](#)]
57. Sadeghilaridjani, M.; Ayyagari, A.; Muskeri, S.; Hasannaemi, V.; Salloom, R.; Chen, W.Y.; Mukherjee, S. Ion irradiation response and mechanical behavior of reduced activity high entropy alloy. *J. Nucl. Mater.* **2020**, *529*, 151955. [[CrossRef](#)]
58. Li, Z.; Pradeep, K.G.; Deng, Y.; Raabe, D.; Tasan, C.C. Metastable high-entropy dual-phase alloys overcome the strength-ductility trade-off. *Nature* **2016**, *534*, 227–230. [[CrossRef](#)] [[PubMed](#)]
59. Li, R.; Wang, Z.; Guo, Z.; Liaw, P.K.; Zhang, T.; Li, L.; Zhang, Y. Graded microstructures of Al-Li-Mg-Zn-Cu entropic alloys under supergravity. *Sci. China Mater.* **2019**, *62*, 736–744. [[CrossRef](#)]
60. Li, R.X.; Liaw, P.K.; Zhang, Y. Synthesis of Al_xCoCrFeNi high-entropy alloys by high-gravity combustion from oxides. *Mater. Sci. Eng. A* **2017**, *707*, 668–673. [[CrossRef](#)]
61. Xing, Q.; Ma, J.; Wang, C.; Zhang, Y. High-Throughput Screening Solar-Thermal Conversion Films in a Pseudobinary (Cr, Fe, V)-(Ta, W) System. *ACS Comb. Sci.* **2018**, *20*, 602–610. [[CrossRef](#)]
62. Parkin, C.; Moorehead, M.; Yu, Z.; Couet, A.; Sridharan, K.; Savan, A.; Ludwig, A.; Zhang, C. Investigation of high-entropy alloys compositions for radiation damage applications. *Trans. Am. Nucl. Soc.* **2018**, *118*, 1583–1586.